THEORETICA CHIMICA ACTA

Theoret. Chim. Acta (Berl.) 51, 297–309 (1979)

Intensity Distribution in the Vibronic Side Bands of the $\Gamma_7(^2T_{2g}) \rightarrow \Gamma_8(^4A_{2g})$ Origin of ReX_6^{2-} Doped K_2PtCl_6-Type Crystals*

Hans Kupka, Rainer Wernicke, Walther Enßlin, and Hans-Herbert Schmidtke

Institut für Theoretische Chemie der Universität Düsseldorf, Universitätsstraße 1, Gebäude 26.32, Ebene 03, D-4000 Düsseldorf 1, Federal Republic of Germany

Intensities of vibronic transitions are calculated using an electronic vibrational coupling scheme of symmetrized and localized interactions. The model consists of an active central ion subject to a valence force field originating from nearest-neighbor displacements. The intensities of vibronic fundamentals are obtained from a generalized Lorentzian line shape function which is applied to the $\Gamma_7(^2T_{2g}) \rightarrow \Gamma_8(^4A_{2g})$ transition of $ReCl_6^{2-}$ and $ReBr_6^{2-}$ in various cubic host crystals A_2MX_6 (A = Rb, Cs; M = Te, Sn, Pb; X = Cl, Br). Relative intensities of the odd vibronic side bands are calculated without knowing actual values for ligand field and spin-orbit coupling parameters, and considering only octahedral vibrational frequencies. The sidebands acquire intensity by a coupling which is cubic in the electron coordinates and linear in the nuclear normal coordinates. With some necessary approximations the present model is able to reproduce the experimental intensity distribution satisfactorily.

Key words: K_2PtCl_6-type crystals, ReX_6^{2-}-doped ~, vibronic band distribution

1. Introduction

In a previous paper the intensity distribution in vibronic progressions such as, for example, those obtained from the phosphorescence spectrum of $ReCl_6^{2-}$ doped in various hexahalogeno-tellurium compounds, has been calculated [1] from a model which considers all interactions between the electronic and vibrational levels, as well as the coupling to the environment, by treating the medium as a heat bath [2]. In this case the spectrum contains some series of vibronically induced $\nu_1(\alpha_{1g})$ progressions associated with the $\nu_2(\varepsilon_g)$, $\nu_3(\tau_{1u})$, $\nu_4(\tau_{1u})$ and $\nu_6(\tau_{2u})$ vibronic origins. The relative intensities of these combination bands with respect to their vibronic

* Dedicated to Professor Dr. H. Hartmann on the occasion of his 65th birthday

0040-5744/79/0051/0297/$02.60

origin lines were expressed by an intramolecular distribution which considers both the effect of geometry and mode frequency changes due to electronic excitation.

In this paper attention is directed to the intensities of the vibronic origins themselves, and in particular to the question of how the intensity is distributed over the most prominent transitions originating from ν_3-, ν_4- and ν_6-normal frequencies which, due to their odd parity, break the selection rule for electric dipole transitions. For this investigation the earlier system can serve again as a good example, since $ReCl_6^{2-}$ and $ReBr_6^{2-}$ doped in antifluorite type host crystals usually supply a very well resolved $\Gamma_7(^2T_{2g}) \rightarrow \Gamma_8(^4A_{2g})$ vibronic spectrum, from which the intensity of each band separately can be determined without difficulty. The host crystals, A_2MX_6 (with A = Rb, Cs; M = Te, Sn, Pb; X = Cl, Br), are known to crystallize over a wide range of temperature in the space group $Fm3m = O_h^5$ [3] in which the Re^{4+} ion takes the position of an exact O_h site as labelled (a) in the international notation. Due to the weak interaction between halogens X and cations A, the ReX_6^{2-} octahedra are considered in the present model as almost isolated molecular entities with internal frequencies not essentially influenced by the cation matrix surroundings. In Fig. 1 the phosphorescence spectrum of $ReCl_6^{2-}$ in Cs_2TeCl_6 at 10 K excited by the 454.5 nm argon laser line is shown, and is characteristic for $\Gamma_7(^2T_{2g}) \rightarrow \Gamma_8(^4A_{2g})$ transitions in these compounds. The sharp peaks at 316, 170 and 134 cm^{-1} on the low energy side of the 0-0 line (at 13865 cm^{-1}) correspond to the ν_3, ν_4, and ν_6 internal modes of the complex octahedron, respectively. The narrow linewidths indicate that the vibrations inducing these transitions must be localized to a great extent. Close to the 0-0 line, which has primarily magnetic dipole character, a group of bands is detected which originate from lattice vibrations. The intensity of these bands is only a few percent of the total integrated absorption. They are, however, not part of this investigation.

The present model uses for the intensity calculation a formula for the generalized Lorentzian line shape function $W(\omega)$ which has been worked out earlier [2]. In this expression an "electron-vibration matrix element" occurs which, from a perturbation treatment, contains all possible interactions between the electronic

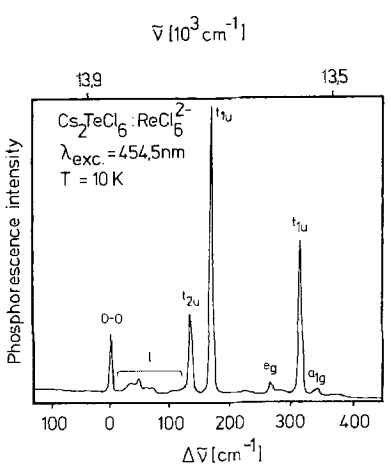

Fig. 1. Emission spectrum of Re^{4+} doped in (a) sites of micro crystalline Cs_2TeCl_6 (space group Fm3m)

states of different multiplicity and different parity due to spin-orbit and electron-vibrational coupling. The latter coupling is calculated from the Herzberg–Teller approximation [4] considering only nearest-neighbor couplings, i.e. the dynamical metal-ligand potential, which is expanded in a series of symmetry adapted spherical harmonics and symmetry coordinates of internal molecular vibrations. Using this expansion some parts of the matrix elements can be calculated, while other parts turn out to be common parameters, e.g. ligand field parameters, which can be determined from the experiment. When replacing the symmetry coordinates by normal coordinates using Wilson's valence force potential [5], a complete diagonalization of the vibrational potential matrix is obtained. Intensity calculations performed by Koide and Pryce [6] on Mn(II) salts using orthogonal, not mass-weighted, coordinates diagonalize the matrix only approximately. The force field of Wilson was used by Liehr and Ballhausen some time ago in their calculation of oscillator strengths of Ti(III) and Cu(II) complexes [7, 8]. Other work related to the present problem or similar phenomena has been done on IrF_6 [9] and on V(II) or Ni(II) in MgO [10, 11]. Also the calculation of Jahn–Teller coupling parameters by Child and Roach on ReF_6, who used a very complicated electric potential between the ligand atoms and the t_{2g} electron, should be mentioned in this context [12].

2. Electric Dipole Transitions

The intensity distribution for the electric dipole transition $\Gamma_7(^2T_{2g}) \rightarrow \Gamma_8(^4A_{2g})$ is given by the generalized Lorentzian line shape function [1, 2] which for y polarization, and considering the odd-parity fundamentals only, is

$$W_y(\omega) = (2\omega^3/3\pi\hbar^2c^3) \sum_{\Gamma_u} \frac{\hbar}{4M_{\Gamma_u}\omega_{\Gamma_u}} \left[\sum_{\gamma_u} \sum_{\gamma_7,\gamma_8} \left| F_{y\Gamma_u\gamma_u}^{\gamma_7 \rightarrow \gamma_8} \right|^2 \right] [\coth(\hbar\omega_{\Gamma_u}/2kT) + 1]$$
$$\cdot \frac{2\vartheta\hbar^{-1}}{(\omega - \Omega + \omega_{\Gamma_u} - \delta_\Gamma)^2 + (\vartheta\hbar^{-1})^2} I_0(0; \Delta_\Gamma, \beta_\Gamma), \tag{1}$$

where

$$I_0(0; \Delta_\Gamma, \beta_\Gamma) = \frac{2\beta_\Gamma^{1/2}}{1 + \beta_\Gamma} \exp\left(-\frac{\beta_\Gamma}{1 + \beta_\Gamma} \Delta_\Gamma^2 \right). \tag{2}$$

For the notation see the earlier work [1, 2]. Equation (1) is also restricted to the Stokes components $\omega = \Omega - \omega_{\Gamma_u} + \delta_\Gamma$ of odd modes. Since the vibrational term $I_0(0; \Delta_\Gamma, \beta_\Gamma)$ is common for all these components, the intensity associated with the Γ_u mode is proportional to the corresponding electronic coupling coefficient (given in the square brackets) and inversely proportional to the product $M_{\Gamma_u}\omega_{\Gamma_u}$ of reduced mass and vibrational angular frequency contributed by this mode. The matrix element for the y-component of the dipole operator, $P_y = e\sum_i y_i$, is

$$F_{y\Gamma_u\gamma_u}^{\gamma_7 \rightarrow \gamma_8} = \sum_{\gamma^*} \sum_{a_i\Gamma_{u_i}} \left[\frac{\langle {}^4A_{2g}\Gamma_8\gamma_8 | P_y | a_i {}^4\Gamma_{u_i}\Gamma^*\gamma^* \rangle \langle a_i {}^4\Gamma_{u_i}\Gamma^*\gamma^* | V_{\Gamma_u\gamma_u} | {}^4T_{2g}\Gamma_7\gamma_7 \rangle}{[E_0({}^2T_{2g}) - E_0({}^4T_{2g})][E_0({}^2T_{2g}) - E_0(a_i {}^4\Gamma_{u_i})]} \right.$$
$$\left. + \frac{\langle {}^4A_{2g}\Gamma_8\gamma_8 | V_{\Gamma_u\gamma_u} | a_i {}^4\Gamma_{u_i}\Gamma^*\gamma^* \rangle \langle a_i {}^4\Gamma_{u_i}\Gamma^*\gamma^* | P_y | {}^4T_{2g}\Gamma_7\gamma_7 \rangle}{[E_0({}^2T_{2g}) - E_0({}^4T_{2g})][E_0({}^4A_{2g}) - E_0(a_i {}^4\Gamma_{u_i})]} \right]$$
$$\cdot \langle {}^4T_{2g}\Gamma_7\gamma_7 | H_{so} | {}^2T_{2g}\Gamma_7\gamma_7 \rangle \tag{3}$$

Table 1. Odd parity symmetry coordinates $S(\Gamma_u\gamma_u)$ of an octahedral MX_6 complex and corresponding spherical harmonics. The central ion is placed at the origin of the coordinate system and the ligands numbered i ($i = 1, 2, 3$) are located on the x, y, and z axes, respectively, and those numbered $i + 3$ are opposite to the central ion. The $\tau_{1u}^{(C)}$ symmetry coordinates are central ion displacements

Representation Γ_u	Symmetry coordinates $S(\Gamma_u\gamma_u)$	Spherical harmonics $Y_l(\theta, \varphi; \Gamma_u\gamma_u)$ $l = 1$	$l = 3$
	$\frac{1}{2}(X_2 + X_3 + X_5 + X_6)$	$\frac{1}{\sqrt{2}}(Y_1^1 - Y_1^{-1})$	$\frac{1}{4}[\sqrt{3}(Y_3^1 - Y_3^{-1}) - \sqrt{5}(Y_3^3 - Y_3^{-3})]$
$\tau_{1u}^{(A)}$	$\frac{1}{2}(Y_1 + Y_3 + Y_4 + Y_6)$	$\frac{1}{\sqrt{2}}i(Y_1^1 + Y_1^{-1})$	$\frac{1}{4}i[\sqrt{3}(Y_3^1 + Y_3^{-1}) + \sqrt{5}(Y_3^3 + Y_3^{-3})]$
	$\frac{1}{2}(Z_1 + Z_2 + Z_4 + Z_5)$	Y_1^0	Y_3^0
	$\frac{1}{\sqrt{2}}(X_1 + X_4)$	$\frac{1}{\sqrt{2}}(Y_1^1 - Y_1^{-1})$	$\frac{1}{4}[\sqrt{3}(Y_3^1 - Y_3^{-1}) - \sqrt{5}(Y_3^3 - Y_3^{-3})]$
$\tau_{1u}^{(B)}$	$\frac{1}{\sqrt{2}}(Y_2 + Y_5)$	$\frac{1}{\sqrt{2}}i(Y_1^1 + Y_1^{-1})$	$\frac{1}{4}i[\sqrt{3}(Y_3^1 + Y_3^{-1}) + \sqrt{5}(Y_3^3 + Y_3^{-3})]$
	$\frac{1}{\sqrt{2}}(Z_3 + Z_6)$	Y_1^0	Y_3^0
	X_0		
$\tau_{1u}^{(C)}$	Y_0		
	Z_0		
	$\frac{1}{2}(X_2 - X_3 + X_5 - X_6)$		$\frac{1}{4}[\sqrt{5}(Y_3^1 - Y_3^{-1}) + \sqrt{3}(Y_3^3 - Y_3^{-3})]$
τ_{2u}	$\frac{1}{2}(Y_3 - Y_1 + Y_6 - Y_4)$		$-\frac{1}{4}i[\sqrt{5}(Y_3^1 + Y_3^{-1}) - \sqrt{3}(Y_3^3 + Y_3^{-3})]$
	$\frac{1}{2}(Z_1 - Z_2 + Z_4 - Z_5)$		$\frac{1}{\sqrt{2}}(Y_3^2 + Y_3^{-2})$

which considers spin-orbit coupling of relevant states of different spin and the mixing of odd parity states $\Gamma_{u_i} = T_{1u_i}$ or T_{2u_i} into the excited state $\Gamma_7(^2T_{2g})$ and the ground state $\Gamma_8(^4A_{2g})$, by virtue of the metal-ligand dynamics. $V_{\Gamma_u\gamma_u}$ results from the Herzberg–Teller approximation [4] and is the derivative of the dynamical ligand potential with respect to the $Q_{\Gamma_u\gamma_u}$ normal coordinate for the ground state equilibrium configuration. If the electron-vibrational coupling is localized in the metal-ligand bond moiety of the complex (nearest neighbor interaction scheme), the vibronic perturbation of the electronic levels due to odd vibrations is given, using symmetry adapted nuclear coordinates $S(\Gamma_u\gamma_u)$, by

$$H_{\mathrm{M-L}} = \sum_i \sum_{l,\Gamma_u} A_l(\Gamma_u) r_i^l \sum_{\gamma_u} Y_l(\theta_i, \varphi_i; \Gamma_u\gamma_u) S(\Gamma_u\gamma_u), \tag{4}$$

where $Y_l(\theta_i, \varphi_i; \Gamma_u\gamma_u)$ are the spherical harmonics of rank l which transform according to the γ_u component of the Γ_u irreducible representation. The position of the d-electron i is given by r_i, θ_i, φ_i. The expansion in the symmetry coordinates is carried out only up to linear terms, since at present we shall neglect all second order couplings. The odd parity nuclear symmetry coordinates of the octahedral complex MX_6, and the corresponding symmetry adapted spherical harmonics, which depend on the electronic coordinates, are listed in Table 1. The coupling coefficients $A_l(\Gamma_u)$ calculated from a Coulomb interaction of effective point-charge q at the ligand are presented for nonvanishing terms (up to fourth order in l) in Table 2. The interaction potential in terms of symmetry coordinates as given in Eq. (4) reduces the number of matrix elements to be calculated substantially.

Table 2. Coupling parameters $A_l(\Gamma_u)$ of an octahedral MX_6 complex (R is the metal-ligand distance)

Representation Γ_u	$A_l(\Gamma_u)\cdot(e\cdot q/R^{l+2})^{-1}$ $l=1$	$l=3$
$\tau_{1u}^{(A)}$	$4\left(\frac{\pi}{3}\right)^{1/2}$	$-6\left(\frac{\pi}{7}\right)^{1/2}$
$\tau_{1u}^{(B)}$	$8\left(\frac{\pi}{6}\right)^{1/2}$	$16\left(\frac{\pi}{14}\right)^{1/2}$
$\tau_{1u}^{(C)}$	$-16\left(\frac{\pi}{3}\right)^{1/2}$	$-4\left(\frac{\pi}{7}\right)^{1/2}$
τ_{2u}		$2\left(\frac{15\pi}{7}\right)^{1/2}$

3. Normal Coordinates

For determining the normal coordinates of the odd vibrations τ_{1u} which occur more than once, the valence force model of Wilson is used

$$2V = K\sum_{i=1}^{6}(\Delta R_i)^2 + 2K_1\sum_{\substack{i,j=1\\ i\neq j}}^{6}(\Delta R_i)(\Delta R_j) + K_\alpha\sum_{i=1}^{12}(R\,\Delta\alpha_i), \tag{5}$$

where the normal vibrational frequencies are given by

$$
\begin{aligned}
&m\lambda_1 = K + 10K_1, \qquad m\lambda_2 = K - 2K_1\\
&m^2\lambda_3\lambda_4 = [(M + 6m)/M](2K_\alpha)(K - 2K_1)\\
&m(\lambda_3 + \lambda_4) = [(M + 4m)/M](2K_\alpha) + [(M + 2m)/M](K - 2K_1)\\
&m\lambda_5 = 4K_\alpha, \qquad m\lambda_6 = 2K_\alpha.
\end{aligned} \tag{6}
$$

K is the M—X force constant, K_1 is the constant for the interaction of two vibrating M—X bonds, and K_α is the constant belonging to the bending of the X—M—X bond. The masses of the central ion and the ligands are M and m, respectively. The λ_i are defined in the usual way [13] $\lambda_i = (2\pi\nu_i)^2 = 4\pi^2c^2\omega_i^2$ where ν_i are normal vibrational frequencies of the complex octahedron. Interactions between ligands of neighboring octahedra, as well as between ligands and the alkali matrix surroundings, are omitted because the corresponding force constants are about 10^3 times smaller than internal force constants of the octahedron [14, 15]. Expanding Eq. (5) as a quadratic form in the τ_{1u} symmetry coordinates and using Eqs. (6), the vibrational potential part in the subspace, belonging to the x component of the τ_{1u} normal coordinates, is

$$
V_{1u} = (S_x^{(A)}, S_x^{(B)}, S_x^{(C)}) \begin{pmatrix} m\lambda_6 & 0 & -2m\lambda_6 \\ 0 & m\lambda_2 & -\sqrt{2}m\lambda_2 \\ -2m\lambda_6 & -\sqrt{2}m\lambda_2 & 2m(\lambda_2 + 2\lambda_6) \end{pmatrix} \begin{pmatrix} S_x^{(A)} \\ S_x^{(B)} \\ S_x^{(C)} \end{pmatrix}. \tag{7}
$$

From a diagonalization of this quadratic form, the following orthogonal transformation to mass-weighted normal coordinates Q_{3x}, Q_{4x} and Q_{trx} is obtained

$$
\begin{aligned}
m^{1/2}S_x^{(A)} &= \frac{2\lambda_6}{\lambda_6 - \lambda_3} N_3 Q_{3x} + \frac{2\lambda_6}{\lambda_6 - \lambda_4} N_4 Q_{4x} + \frac{2}{(6 + M/m)^{1/2}} Q_{trx}\\
m^{1/2}S_x^{(B)} &= \frac{\sqrt{2}\lambda_2}{\lambda_2 - \lambda_3} N_3 Q_{3x} + \frac{\sqrt{2}\lambda_2}{\lambda_2 - \lambda_4} N_4 Q_{4x} + \frac{\sqrt{2}}{(6 + M/m)^{1/2}} Q_{trx}\\
M^{1/2}S_x^{(C)} &= (M/m)^{1/2}(N_3 Q_{3x} + N_4 Q_{4x}) + \left(\frac{M/m}{6 + M/m}\right)^{1/2} Q_{trx}
\end{aligned} \tag{8}
$$

with

$$
N_3 = \frac{1}{\left[\left(\frac{2\lambda_6}{\lambda_6 - \lambda_3}\right)^2 + \left(\frac{\sqrt{2}\lambda_2}{\lambda_2 - \lambda_3}\right)^2 + M/m\right]^{1/2}}
$$

and

$$
N_4 = \frac{1}{\left[\left(\frac{2\lambda_6}{\lambda_6 - \lambda_4}\right)^2 + \left(\frac{\sqrt{2}\lambda_2}{\lambda_2 - \lambda_4}\right)^2 + M/m\right]^{1/2}}. \tag{9}
$$

The orthogonal transformation, Eq. (8), differs from that used by Koide and Pryce [6] in that it contains the normal vibrational frequencies of the octahedral complex, due to the solution of the eigenvalue problem of Eq. (7). The τ_{1u} normal coordinates,

Q_{sx} ($s = 3, 4$), and the pure translational coordinate, Q_{trx}, of the entire octahedron are obtained from the inverse of Eq. (8). Using Eq. (8) in Eq. (4), the coupling between electronic motion and odd nuclear vibrations through the operator $V_{\Gamma_u\gamma_u}$, is

$$H_{\text{M-L}} = V_{3x}Q_{3x} + V_{4x}Q_{4x} + V_{6x}Q_{6x} + \cdots, \tag{10}$$

where

$$V_{3x} = \frac{N_3}{m^{1/2}} \sum_{i=1}^{3} \left\{ \sum_l \left[A_l(\tau_{1u}^{(A)}) \frac{2\lambda_6}{\lambda_6 - \lambda_3} + A_l(\tau_{1u}^{(B)}) \frac{\sqrt{2}\lambda_2}{\lambda_2 - \lambda_3} + A_l(\tau_{1u}^{(C)}) \right] \cdot r_i^l Y_l(\theta_i, \varphi_i; \tau_{1u}x) \right\}$$

$$V_{4x} = \frac{N_4}{m^{1/2}} \sum_{i=1}^{3} \left\{ \sum_l \left[A_l(\tau_{1u}^{(A)}) \frac{2\lambda_6}{\lambda_6 - \lambda_4} + A_l(\tau_{1u}^{(B)}) \frac{\sqrt{2}\lambda_2}{\lambda_2 - \lambda_4} + A_l(\tau_{1u}^{(C)}) \right] \cdot r_i^l Y_l(\theta_i, \varphi_i; \tau_{1u}x) \right\}$$

$$V_{6x} = \sum_{i=1}^{3} \left\{ \sum_l A_l(\tau_{2u}) r_i^l Y_l(\theta_i, \varphi_i; \tau_{2u}x) \right\}$$

$$V_{trx} = 0. \tag{11}$$

It is worth noting that, for the vibrational frequencies of present interest, the normal mode Q_3 represents predominantly ligand-metal stretching vibrations, whereas Q_4 involves stretching and angular vibrations.

In a similar way the y- and z-components of the V coupling coefficients are obtained by using in Eqs. (11) spherical harmonics. $Y_l(\theta, \varphi; \Gamma_u\gamma_u)$ (from Table 1) belonging to the other coordinates.

4. Calculation of the Intensity Matrix Elements

For evaluating the intensities some approximations in the transition matrix element, Eq. (3), must be made. Since all intermediate odd-parity electronic states Γ_{u_i} result from an electron transfer from the ligands to the partly filled d shell of the central atom [16], these states should lie much higher than the ligand field states $^2T_{2g}$ and $^4A_{2g}$. Under this condition the denominators of Eq. (3) may be considered as independent from i and replaced by a common parameter $(\Delta E)^2$. Since the odd parity states Γ_{u_i} appear as projection operator expressions which transform as the totally symmetric representation in the point group O_h, the closure property

$$\sum_{a_i, \gamma^*} |a_i\, {}^4\Gamma_{u_i}\Gamma^*\gamma^*\rangle\langle a_i\, {}^4\Gamma_{u_i}\Gamma^*\gamma^*| = 1 \tag{12}$$

can be applied. This leads to the much simpler form

$$F_{y\Gamma_u\gamma_u}^{\gamma_7 \to \gamma_8} = \frac{2}{(\Delta E)^2} \langle {}^4A_{2g}\Gamma_8\gamma_8 | P_y V_{\Gamma_u\gamma_u} | {}^4T_{2g}\Gamma_7\gamma_7 \rangle \langle {}^4T_{2g}\Gamma_7\gamma_7 | H_{so} | {}^2T_{2g}\Gamma_7\gamma_7 \rangle. \tag{13}$$

The calculation of Eq. (13) requires the electronic wave functions $|^4A_{2g}\Gamma_8\rangle$, $|^2T_{2g}\Gamma_7\rangle$ and $|^4T_{2g}\Gamma_7\rangle$. Two functions belonging to the lowest energy states are obtained [17] from a crystal field diagonalization of the Eisenstein energy matrices [18]

$$\begin{aligned} |^4A_{2g}\Gamma_8\rangle &= 0.97|\Gamma_8(^4A_{2g}t_{2g}^3)\rangle + 0.2|\Gamma_8(^2T_{2g}t_{2g}^3)\rangle \\ |^2T_{2g}\Gamma_7\rangle &= 0.98|\Gamma_7(^2T_{2g}t_{2g}^3)\rangle + 0.13|\Gamma_7(^4T_{2g}t_{2g}^2e_g)\rangle \end{aligned} \tag{14}$$

which indicates that they have primarily $^4A_{2g}(\Gamma_8)$ and $^2T_{2g}(\Gamma_7)$ character, respectively. In the following calculation only the main parts of the eigenfunctions (Eq. (14)) are used. The same assumption will be made concerning the $^4T_{2g}(\Gamma_7)$ character of the first intermediate electronic state $|^4T_{2g}\Gamma_7\rangle$. Using the fact that the spin-orbit matrix element, $\Xi = \langle^4T_{2g}\Gamma_7\gamma_7|H_{so}|^2T_{2g}\Gamma_7\gamma_7\rangle$, does not depend on the γ_7 component, the transition matrix element becomes

$$F_{y\Gamma_u\gamma_u}^{\gamma_7\to\gamma_8} = \frac{\Xi}{(\Delta E)^2}\sum_{\gamma_{2g}} F_{y\Gamma_u\gamma_u}^{\gamma_{2g}}\Pi\gamma_{2g}(\gamma_7, \gamma_8) \tag{15}$$

with

$$F_{y\Gamma_u\gamma_u}^{\gamma_{2g}} = \langle^4A_{2g}a_2|P_yV_{\Gamma_u\gamma_u}|^4T_{2g}\gamma_{2g}\rangle \tag{16}$$

and the coefficients being

$$\Pi\gamma_{2g}(\gamma_7, \gamma_8) = \sum_{\gamma_s}\langle\tfrac{3}{2}A_{2g}\Gamma_8\gamma_8|\tfrac{3}{2}A_{2g}a_2\gamma_s\rangle\langle\tfrac{3}{2}T_{2g}\gamma_{2g}\gamma_s|\tfrac{3}{2}T_{2g}\Gamma_7\gamma_7\rangle \tag{17}$$

which are listed in Table 3.

In order to evaluate the matrix elements of Eq. (16) we consider the integrals

$$W_{y\Gamma_u\gamma_u}^{\gamma_{2g}} = \langle^4A_{2g}a_2|P_y\sum_i r_i^l Y_l(\theta_i, \varphi_i; \Gamma_u\gamma_u)|^4T_{2g}\gamma_{2g}\rangle, \tag{18}$$

Table 3. Nonvanishing coefficients $\Pi\gamma_{2g}(\gamma_7, \gamma_8)$

	Π_ξ		Π_ζ	
γ	α	β	α	β
κ	$\frac{i}{2\sqrt{3}}$		$\frac{i}{\sqrt{3}}$	
λ		$-\frac{i}{2}$		$\frac{i}{\sqrt{3}}$
μ	$\frac{i}{2}$			
ν		$-\frac{i}{2\sqrt{3}}$		

which arise from Eq. (16) by introducing Eq. (11). From symmetry considerations, the nonvanishing components of $W^{\gamma_{2g}}_{y\Gamma_u\gamma_u}$ are those which have $\gamma_{2g} = \xi, \zeta$ of ${}^4T_{2g}$, and the only integrals to be calculated are

$$\begin{aligned} W^{\xi}_{y\Gamma_u\gamma_u} &= \langle {}^4T_{2g}\xi | P_y \sum_i r_i^l Y_l(\Gamma_u\gamma_u) | {}^4A_{2g}a_2\rangle, \quad \text{for } \Gamma_u\gamma_u = \tau_{1u}z \text{ and } \tau_{2u}\zeta \\ W^{\zeta}_{y\Gamma_u\gamma_u} &= \langle {}^4T_{2g}\zeta | P_y \sum_i r_i^l Y_l(\Gamma_u\gamma_u) | {}^4A_{2g}a_2\rangle, \quad \text{for } \Gamma_u\gamma_u = \tau_{1u}x \text{ and } \tau_{2u}\xi \end{aligned} \tag{19}$$

where, for simplicity, the electron coordinate labels are omitted in the spherical harmonics. The components of ${}^4T_{2g}$ are ξ, η, ζ, which transform like zy, xz, xy, respectively; a_2 indicates the single component of the ground state ${}^4A_{2g}$.

The electronic basis functions for $M_s = \frac{3}{2}$ in terms of Heisenberg–Slater determinants in the strong field case are [19]

$$\begin{aligned} |{}^4A_{2g}a_2\rangle &= -|\xi\eta\zeta| \\ |{}^4T_{2g}\xi\rangle &= \tfrac{1}{2}\{\sqrt{3}|\eta\zeta u| + |\eta\zeta v|\} \\ |{}^4T_{2g}\eta\rangle &= \tfrac{1}{2}\{-\sqrt{3}|\zeta\xi u| + |\zeta\xi v|\} \\ |{}^4T_{2g}\zeta\rangle &= -|\xi\eta v|. \end{aligned} \tag{20}$$

Introducing Eq. (20) into Eqs. (18) and (19) yields

$$\begin{aligned} W^{\xi}_{y\Gamma_u\gamma_u} &= -\tfrac{1}{2}e\langle v | y\cdot r^l Y_l(\Gamma_u\gamma_u)|\xi\rangle - \frac{\sqrt{3}}{2} e\langle u | y\cdot r^l Y_l(\Gamma_u\gamma_u)|\xi\rangle, \\ \Gamma_u\gamma_u &= \tau_{1u}z,\ \tau_{2u}\zeta \\ W^{\zeta}_{y\Gamma_u\gamma_u} &= e\langle\zeta | y\cdot r^l Y_l(\Gamma_u\gamma_u)|v\rangle, \qquad \Gamma_u\gamma_u = \tau_{1u}x,\ \tau_{2u}\xi. \end{aligned} \tag{21}$$

Evaluating the one-electron matrix elements finally results in

$$\begin{aligned} l = 1 \qquad & W^{\zeta}_{y\tau_{1u}x} = W^{\xi}_{y\tau_{1u}z} = 0 \\ & W^{\zeta}_{y\tau_{2u}\xi} = W^{\xi}_{y\tau_{2u}\zeta} = 0 \\ l = 3 \qquad & W^{\zeta}_{y\tau_{1u}x} = -W^{\xi}_{y\tau_{1u}z} = \frac{5}{3\cdot 4\cdot 7}\left(\frac{7}{\pi}\right)^{1/2} e\langle r^4\rangle \\ & W^{\zeta}_{y\tau_{2u}\zeta} = W^{\xi}_{y\tau_{2u}\zeta} = -\frac{1}{4}\left(\frac{5}{21\pi}\right)^{1/2} e\langle r^4\rangle. \end{aligned} \tag{22}$$

From this, it follows that no dipole terms ($l = 1$) contribute to any transition probability component (Eq. (1)). The first nonvanishing matrix elements arise from octopole ($l = 3$) terms, i.e. the one-phonon side band can be considered as originating from a coupling which is linear in the nuclear coordinates and cubic in the electronic coordinates. Although some contribution is also expected from the $l = 5$ terms [6], the dominant contribution to the transition probability is expected from the $l = 3$ terms [11].

Employing Eqs. (18) and (22) in Eq. (13) the sums of squares of electronic coupling factors are as follows

$$\sum_{\gamma_7,\gamma_8} |F^{\gamma_7\to\gamma_8}_{y\tau^{(3)}_{1u}z}|^2 = \frac{4}{3}\frac{N_3}{m}\frac{\Xi^2}{(\Delta E)^4}\left[A_3(\tau^{(A)}_{1u})\frac{2\lambda_6}{\lambda_6-\lambda_3} + A_3(\tau^{(B)}_{1u})\frac{\sqrt{2}\lambda_2}{\lambda_2-\lambda_3} + A_3(\tau^{(C)}_{1u})\right]^2 \cdot |W^{\zeta}_{y\tau_{1u}x}|^2$$

$$\sum_{\gamma_7,\gamma_8} |F^{\gamma_7\to\gamma_8}_{y\tau^{(4)}_{1u}z}|^2 = \frac{4}{3}\frac{N_4}{m}\frac{\Xi^2}{(\Delta E)^4}\left[A_3(\tau^{(A)}_{1u})\frac{2\lambda_6}{\lambda_6-\lambda_4} + A_3(\tau^{(B)}_{1u})\frac{\sqrt{2}\lambda_2}{\lambda_2-\lambda_4} + A_3(\tau^{(C)}_{1u})\right]^2 \cdot |W^{\zeta}_{y\tau_{1u}x}|^2$$

$$\sum_{\gamma_7,\gamma_8} |F^{\gamma_7\to\gamma_8}_{y\tau_{2u}\zeta}|^2 = \frac{4}{3}\frac{\Xi^2}{(\Delta E)^4}|A_3(\tau_{2u})W^{\zeta}_{y\tau_{2u}\xi}|^2. \tag{23}$$

Contributions of $\tau_{1u}x$ or $\tau_{2u}\xi$ components are equal, since for symmetry reasons $|F_{y\tau_{1u}z}| = |F_{y\tau_{1u}x}|$ and $|F_{y\tau_{2u}\zeta}| = |F_{y\tau_{2u}\xi}|$. The ligand mass m appears in Eqs. (23) for the two τ_{1u} modes since the normal coordinates Q_{3x} and Q_{4x}, obtained from the inverse transformation of Eq. (8), have mass adjusted scales. On multiplying, according to Eq. (1), the electronic coupling factors of Eq. (23) by $\hbar/4\omega_3$, $\hbar/4\omega_4$ and $\hbar/4m\omega_6$, respectively, the relative intensities for the fundamental vibronic lines $\nu_3(\tau^{(3)}_{1u})$, $\nu_4(\tau^{(4)}_{1u})$ and $\nu_6(\tau_{2u})$ are obtained.

5. Numerical Results and Comparison with the Experiment

The integrated intensities of vibronic transitions are linearly proportional to the electronic coupling factors, Eq. (23), and are calculated using coupling coefficients $A_i(\Gamma_u)$ of Table 2

$$I(\nu_3) \propto \frac{\hbar}{m\omega_3}\frac{\Xi^2}{(\Delta E)^4}\left(\frac{10\mathrm{Dq}}{28}\right)^2 \frac{\left[-12\frac{\lambda_6}{\lambda_6-\lambda_3} + 16\frac{\lambda_2}{\lambda_2-\lambda_3} - 4\right]^2}{\left(\frac{2\lambda_6}{\lambda_6-\lambda_3}\right)^2 + \left(\frac{\sqrt{2}\lambda_2}{\lambda_2-\lambda_3}\right)^2 + \frac{M}{m}}$$

$$I(\nu_4) \propto \frac{\hbar}{m\omega_4}\frac{\Xi^2}{(\Delta E)^4}\left(\frac{10\mathrm{Dq}}{28}\right)^2 \frac{\left[-12\frac{\lambda_6}{\lambda_6-\lambda_4} + 16\frac{\lambda_2}{\lambda_2-\lambda_4} - 4\right]^2}{\left(\frac{2\lambda_6}{\lambda_6-\lambda_4}\right)^2 + \left(\frac{\sqrt{2}\lambda_2}{\lambda_2-\lambda_4}\right)^2 + \frac{M}{m}} \tag{24}$$

$$I(\nu_6) \propto \frac{\hbar}{m\omega_6}\frac{\Xi^2}{(\Delta E)^4}\,36\left(\frac{10\mathrm{Dq}}{28}\right)^2$$

where the common ligand field parameter of cubic symmetry

$$\mathrm{Dq} = \frac{1}{6}\frac{e\cdot q}{R^5}\langle r^4\rangle \tag{25}$$

is introduced.

The resulting formulae, Eq. (24), supply detailed information on the mechanism of the $\Gamma_7(^2T_{2g}) \to \Gamma_8(^4A_{2g})$ transition. As expected, all intensities increase for a larger spin-orbit coupling and decrease strongly with higher energy gaps to the odd

Table 4. Experimental normal vibrational frequencies (in cm^{-1}) of the ReX_6^{2-} complexes in several crystal hosts, from luminescence spectra at various temperatures T. For experimental details see Ref. [1]

Compound	ν_2	ν_3	ν_4	ν_6	T
$Rb_2TeCl_6:ReCl_6^{2-}$	279	326	168	128	10 K
$Cs_2TeCl_6:ReCl_6^{2-}$	265	316	170	134	10 K
$Rb_2SnCl_6:ReCl_6^{2-}$	287[a]	312	167	131	85 K
$Cs_2SnCl_6:ReCl_6^{2-}$	287[a]	306	171	136	85 K
$Rb_2PbCl_6:ReCl_6^{2-}$	294	322	169	131	85 K
$Cs_2PbCl_6:ReCl_6^{2-}$	282	315	170	138	85 K
$Rb_2SnBr_6:ReBr_6^{2-}$	190	219	113	81	10 K
$Cs_2SnBr_6:ReBr_6^{2-}$	188	216	114	86	10 K

[a] From Ref. [20].

intermediate electronic states. However, intensities increase with the square of the ligand field parameter. A numerical evaluation of the rather complex frequency factor indicates that angular vibrations obviously contribute more to the intensity gain than does the τ_{1u} stretching mode. The displacement of the central ion, on the other hand, is less effective for promoting these transitions.

The experimental normal frequencies determined from the luminescence spectrum of some ReX_6^{2-} doped host crystals are compiled in Table 4. They are used in the calculation of relative intensities according to the present procedure. In Table 5 both the calculated and experimental intensity ratios, $I(\nu_i)/I(\nu_4)$, are given. The agreement is actually very good for the τ_{1u} vibronic intensities. For τ_{2u}, however, the calculated intensities differ appreciably from the experimental. The discrepancy arises from the neglect of any differences in the energy denominators for different odd parity states Γ_{u_i} compared to the ligand field states. This approximation, which is usually made in intensity calculations of this kind, is obviously too severe.

In all hexahalogeno complexes the vibronic sideband of highest intensity is the ν_4

Table 5. Calculated and experimental (in brackets) ratios of integrated intensity for vibrations ν_6, ν_4 and ν_3

Compound	$I(\nu_6)/I(\nu_4)$	$I(\nu_3)/I(\nu_4)$	T
$Rb_2TeCl_6:ReCl_6^{2-}$	0.59 (0.25)[a]	0.66 (0.44)	10 K
$Cs_2TeCl_6:ReCl_6^{2-}$	0.54 (0.27)	0.59 (0.56)	10 K
$Rb_2SnCl_6:ReCl_6^{2-}$	0.53 (0.36)	0.78 (0.62)	85 K
$Cs_2SnCl_6:ReCl_6^{2-}$	0.54 (0.35)	0.85 (0.65)	85 K
$Rb_2PbCl_6:ReCl_6^{2-}$	0.60 (0.38)	0.82 (0.47)	85 K
$Cs_2PbCl_6:ReCl_6^{2-}$	0.56 (0.38)	0.78 (0.67)	85 K
$Rb_2SnBr_6:ReBr_6^{2-}$	0.52 (0.33)	0.66 (0.76)	10 K
$Cs_2SnBr_6:ReBr_6^{2-}$	0.50 (0.36)	0.67 (0.86)	10 K

[a] The experimental data are in error of about 5%.

vibration, which corresponds to a simultaneous stretching and angular vibrational mode. The intensity of the ν_3 vibration, which is almost entirely a metal-ligand stretching mode, leading to a dipolar field at the active ion, is found to be smaller by a factor of approximately two, compared to the ν_4 peak. This intensity relation seems to be reasonable in view of the fact that the inversion center is destroyed more effectively by an angular vibration than by a distortion due to various bond stretches. On the other hand, the ν_3 line is generally stronger than the ν_6 line, the intensity of the latter being induced by a purely angular vibrational mode of the ligands. In $MgO:Cr^{3+}$ Manson and Shah [21] measured a larger ν_6 intensity compared to the total of ν_4 and ν_3 intensities. They explain this unusual finding by the effect of dipole fields in higher order which in τ_{1u} vibrations may have opposite sign to the coupling effect through the octopole field, yielding a lower overall intensity for ν_4 and ν_3 bands. It should, however, be mentioned that oxides do not represent a very good example for a calculation of the present kind since, due to the broadness of the bands, a much larger coupling of the internal modes to the phonon field of the crystal must be assumed as compared to the systems considered in the present work.

6. Conclusion

A calculation of relative intensities of vibrationally induced electric dipole transitions between states resulting from the same electronic configuration of octahedral complex compounds yields the correct order of magnitude. The model starts from the formulae derived earlier for the line shape functions which, for carrying out computations, have to be simplified by introducing some physically reasonable assumptions. The result supplies further insight into the "intensity borrowing mechanism" due to the intramolecular coupling of electronic and nuclear energy levels which, by numerical computation of different contributions, is investigated more quantitatively.

Acknowledgement. Financial support of the Deutsche Forschungsgemeinschaft, Bonn-Bad Godesberg, is gratefully acknowledged.

References

1. Kupka, H., Enßlin, W., Wernicke, R., Schmidtke, H.-H.: Mol. Phys., in print
2. Kupka, H.: Mol. Phys. **36**, 685 (1978)
3. Wyckoff, R. G.: Crystal structures, Vol. 3. New York: Wiley 1965
4. Herzberg, G., Teller, E.: Z. Physik. Chem. B **21**, 410 (1933)
5. Yost, D. M., Steffens, C. C., Gross, S. T.: J. Chem. Phys. **2**, 311 (1934)
6. Koide, S., Pryce, M. H. L.: Phil. Mag. **3**, 607 (1958)
7. Liehr, A. D., Ballhausen, C. J.: Phys. Rev. **106**, 1161 (1957)
8. Liehr, A. D., Ballhausen, C. J.: Ann. Phys. (N.Y.) **3**, 304 (1958)
9. Brand, J. C. D., Goodman, G. L., Weinstock, B.: J. Mol. Spectry. **37**, 464 (1971)
10. Sangster, M. J. L., McCombie, C. W.: J. Phys. C **3**, 1498 (1970)
11. Manson, N. B.: Phys. Rev. B **4**, 2645 (1971)
12. Child, M. S., Roach, A. C.: Mol. Phys. **9**, 281 (1965)

13. Wilson, E. B., Decius, J. C., Cross, P. C.: Molecular vibrations, The theory of infrared and Raman vibrational spectra. New York: McGraw-Hill Book Company 1955
14. O'Leary, P. G., Wheeler, I. D.: Phys. Rev. B **1**, 4909 (1970)
15. Berg, R. W., Poulsen, F. W., Bjerrum, N. J.: J. Chem. Phys. **67**, 1829 (1977)
16. Jørgensen, C. K.: Advan. Chem. Phys. **5**, 33 (1963)
17. Dorain, P. B.: Transition Metal Chem. **4**, 1 (1968)
18. Eisenstein, J.: J. Chem. Phys. **34**, 1628 (1961)
19. Sugano, S., Tanabe, Y., Kamimura, H.: Multiplets of transition metal ions in crystals. New York–London: Academic Press 1970
20. Black, A. M., Flint, C. D.: J. Chem. Soc. Faraday II, **73**, 877 (1977)
21. Manson, N. B., Shah, G. A.: J. Phys. C **10**, 1991 (1977)

Received November 21, 1978